

CONF-86/176-2

BNL 38900

BNL--38900

DE87 003195

NEUTRON RESONANCE AVERAGING

Robert E. Chrien

Brookhaven National Laboratory

Abstract: The principles of resonance averaging as applied to neutron capture reactions are described. Several illustrations of resonance averaging to problems of nuclear structure and the distribution of radiative strength in nuclei are provided.

I. Introduction

The ideas of resonance averaging, especially as applied to neutron induced reactions, are quite old. Averaging can result implicitly, as in the recording of microscopic cross section with low resolution compared to the level spacing, i.e.  $R > D$ , or explicitly, as in the case of high resolution measurements of discrete resonances, where the averaging is done numerically after the fact of measurement. In principle, it is always better to measure fine structure data, in that more information is available. For example, initial states can be segregated according to spin-parity. For the measurement of neutron strength functions, which are related to average cross sections in the cloudy-crystal-ball model, separation into  $l=0, 1, 2$  components is easiest when the fine structure data are available.

Weidenmüller<sup>1</sup> has recently stressed the fact that it is only these average quantities (strength functions) which are of physical significance. The fluctuations from the averages can be successfully treated as statistical fluctuations within the framework of Porter-Thomas analysis. While this view is unpalatable to many of us who have spent much effort in measuring the widths of fine structure resonances, the weight of experimental evidence supports Weidenmüller's contention. In any case, in this review, it is the average quantities which will be addressed, and, in particular, the photon strength function.

II. Technique

An experimental technique for direct averaging requires a well-defined, and not too broad, distribution of incident neutron energies. Another requirement is a sufficient beam intensity coupled with a good suppression of background neutrons. Such a beam can be produced by combining the properties of a source with a transmission filter of some kind; so that the capture reactions are confined to a suitably narrow and well-defined energy region. It has turned out that, because of the intensity requirement, a reactor neutron source is the best choice for direct

**MASTER**

*Isue*

averaging. There are three such sources which have been used for this purpose: 1) the  $^{10}\text{B}$  filtered internal target source at the Argonne CP-5 Reactor; the 2 keV scandium filtered beam, and 3) the 24.3 keV iron (or  $^{56}\text{Fe}$ ) filtered beam.

These facilities have been described in detail<sup>2-3</sup>. Here I merely summarize the spectral properties of these sources. They are shown in Fig. 1.

The  $E^{-1/2}$  characteristic of a boron filter combined with the  $E^{-1}$  reactor spectrum serves to produce the broadly-peaked distribution of 1a. The roughly  $1/v$  capture cross section characteristic of most target further narrows the range of capture events as shown in 1a. Notice that although a broad range of neutron energies is captured, the range is sufficiently narrow compared to the typical germanium response function. Thus the detector response is only slightly degraded. For both the scandium and Fe filters, the averaging interval is more precisely defined at the major interference windows near 2 and 24.3 keV.

Data from capture in discrete resonances is important in the interpretation of averaged spectra for the following reason: The measurement of discrete resonance partial widths can yield absolute values of the widths. These can serve to normalize the intensities observed in resonance averaged capture and thus permit the extraction of absolute averaged widths or strength functions. The absolute strength functions for discrete resonance capture measured at the Brookhaven National Laboratory High Flux Beam Reactor (HFBR) are summarized in Ref. 4.

Over the past decade, slow but steady progress has been made on the development of high resolution and high efficiency intrinsic germanium detectors. The spectrometer in current use at the HFBR is an improved version of the design of Stelts<sup>5-6</sup>, and is currently in use for resonance averaged measurements at 2 and 24.3 keV at the HFBR. Figure 3a,b summarizes the presently available resolution and efficiency on the 3-crystal pair spectrometer shown in Fig. 2. To give an impression of the quality of the spectra obtainable, the 2 and 24 keV capture data from  $^{188}\text{Os}(n,\gamma)^{189}\text{Os}$  are shown in Figs. 4a, b, each taking 10 days at the HFBR, with a sample size of 15.5 gms (2.4 gms/cm<sup>2</sup>).<sup>6</sup> For the HFBR facility the beam strength is typically  $10^7$  neutrons/sec falling on a 2.54 cm x 2.54 cm area. While this is low compared to thermal neutron beams, it is high enough to produce useful results even for small samples.

### III. Analysis of Resonance Averaging

It is well known that the distribution of resonance partial radiative widths follows, to a good approximation, a Porter-Thomas function, that is

$$P(x) = [2\Gamma(1/2)]^{-1} x^{-1/2} e^{-x/2} \quad (1)$$

for  $x = \Gamma/\langle\Gamma\rangle$ . This is expected from the concept of a statistical compound nucleus. While deviations from the above have frequently been claimed, there is

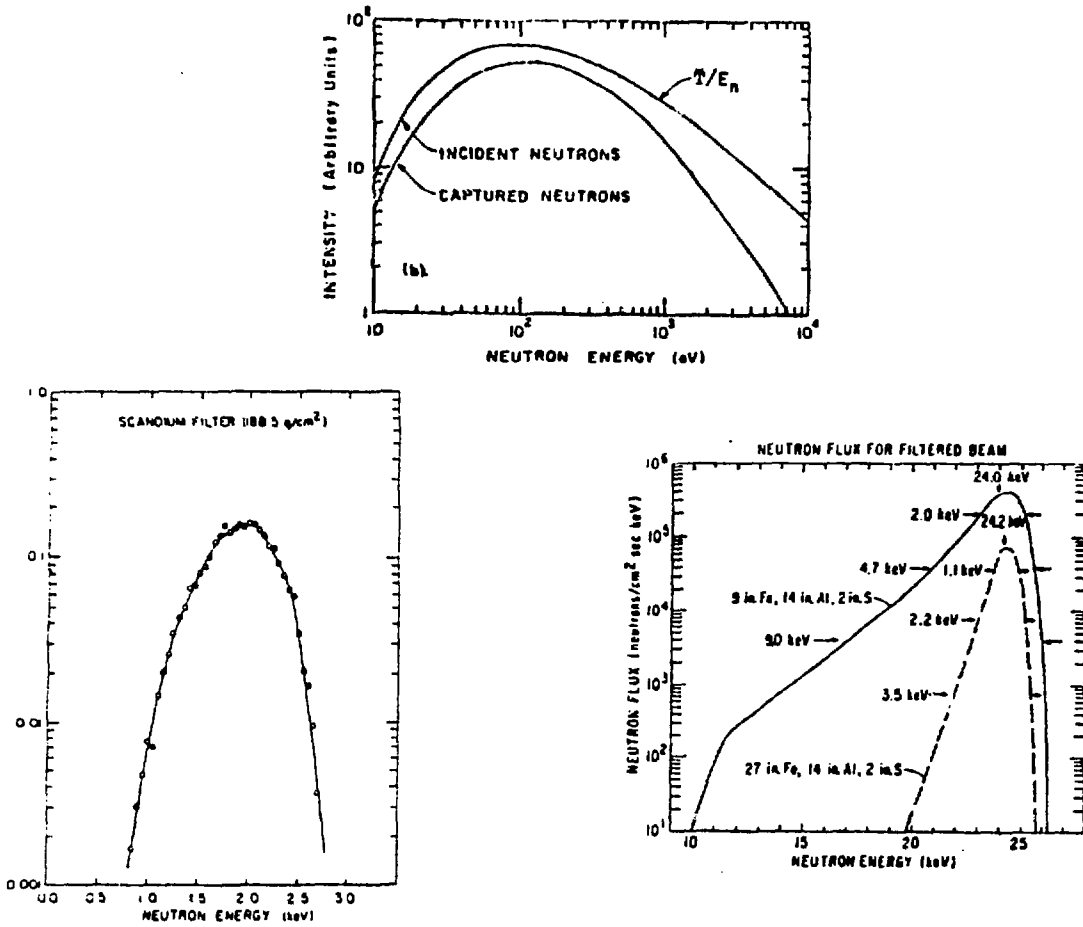


Fig. 1 Spectral distributions for neutron sources at a)  $\approx 150$  eV, b) 2 keV, and c) 24 keV.

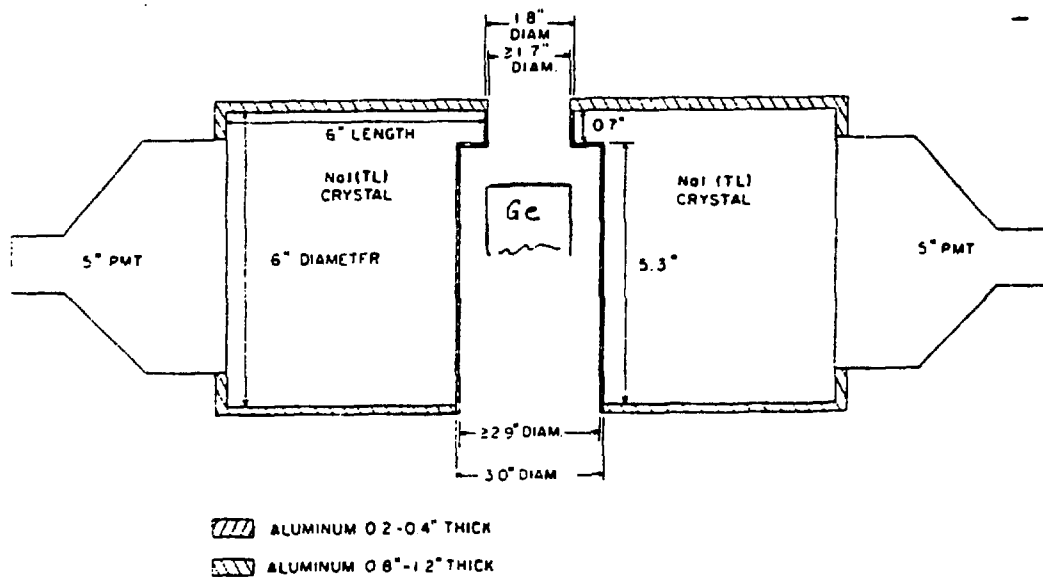


Fig. 2 A sketch of the pair spectrometer used for resonance averaging at the HFBR.

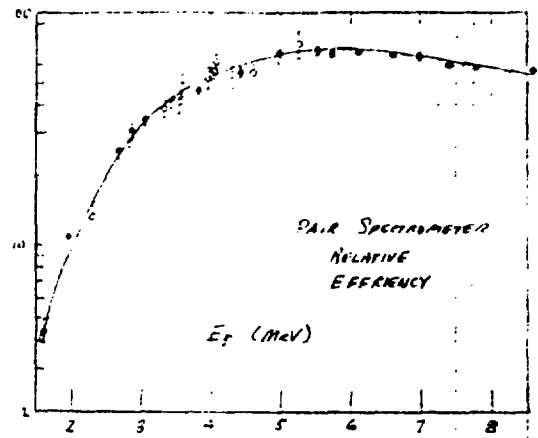
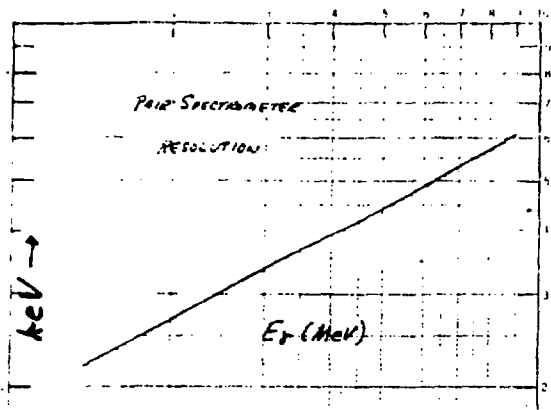


Fig. 3 Resolution (a) and efficiency (b) graphs for the 3-crystal pair spectrometer of Fig. 2.

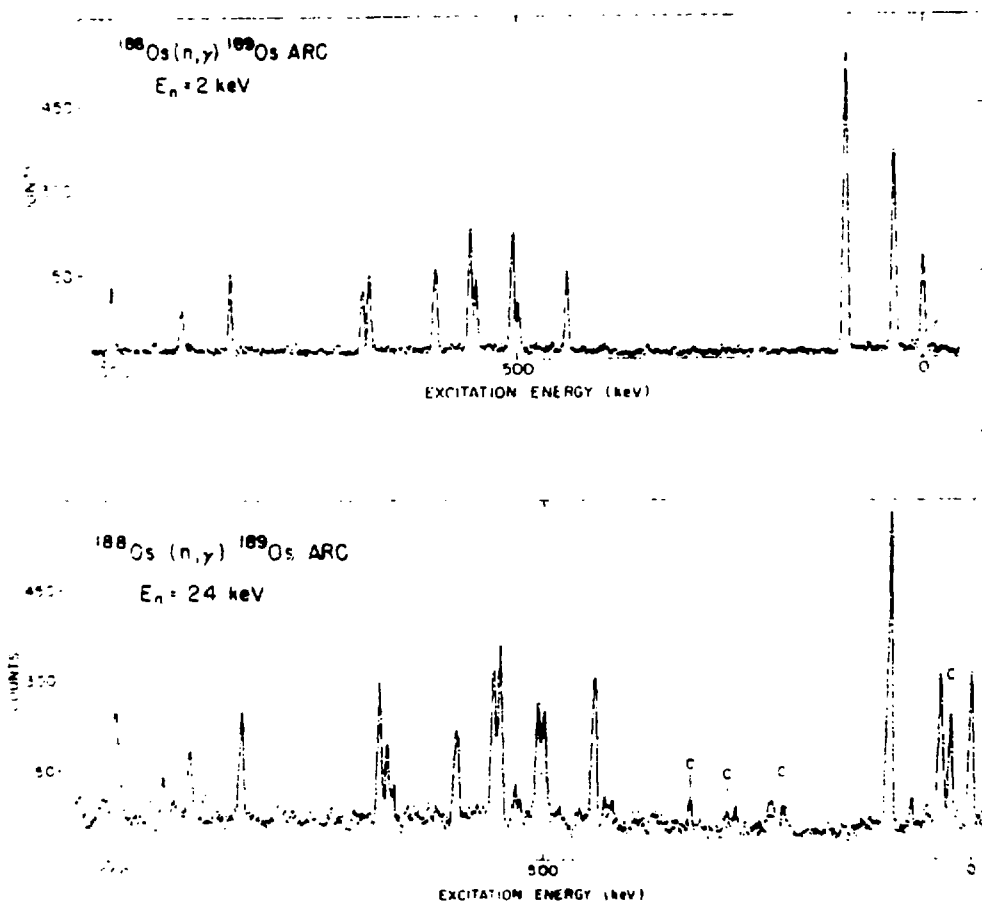


Fig. 4 An example of typical 2 and 24 keV spectra taken at the HFBR.

little evidence for a global violation. The usefulness of resonance averaging follows directly from the properties of an ensemble of Porter-Thomas variables. Averaging over a collection of such variables reduces their dispersion dramatically, and, in the limit, the relative variance approaches  $2/n$ . As pointed out by Bollinger<sup>7</sup> in 1966, if the dispersion after averaging is small enough, primary  $\gamma$ -ray transitions will divide into intensity groups according simply to the number of ways, or paths, for the population of the final states. The paths are determined by the photon selection rules and final state spins and parities. The illustration of Fig. 5 makes the point intuitively obvious. (These remarks are qualitative and apply only to the limit of low energy, more precisely when  $\Gamma_\gamma \gg \Gamma_n$ .)

These ideas can be made more precise by considering the expression for the capture cross section<sup>8</sup>,

$$\sigma = 2\pi^2 k^2 \sum_{J\lambda} g_J \rho_J \langle (\Gamma_n \Gamma_{\lambda if} / \Gamma) \rangle \quad (2)$$

where  $\rho_J = \rho_0(2J+1)\exp[-J(J+1)/2\sigma^2]$

and  $\rho_J$  is the level density, and  $\sigma$  of the spin cut-off parameter. Performing a suitable average over the Porter-Thomas variables introduced to represent the partial widths  $\Gamma_n$ ,  $\Gamma_{\lambda if}$ , is necessary. This is conveniently done, for example, by the Monte Carlo computer code "RACA" (Resonance Averaged Capture Analysis)<sup>9-10</sup>. As a practical matter, a number of assumptions have to be introduced to implement the averaging. The major assumptions are these:

- 1) D-wave (and higher- $\lambda$ ) neutron capture is neglected.
- 2) Quadrupole (and higher L) radiative transitions are negligible.
- 3) Neutron and photon strength functions are presumed to be spin (and channel spin) independent.
- 4) Reduced neutron and radiative widths are Porter-Thomas variables.
- 5) Total radiative widths are constant and spin-parity independent from resonance to resonance.

An important further assumption must be introduced if the data are descriptive of a broad region of nuclear excitation energy. That assumption concerns the energy dependence of the photon strength functions. At this point it is useful to draw attention to one of the classical unsolved problems of nuclear physics. The problem was pointed out by Brink<sup>11</sup> in 1955: the calculation of the size of slow neutron radiative widths. Brink, aware of the fact that the E-1 radiative strength in nuclei tended to cluster in a giant resonance centered eight-to-ten MeV above the neutron separation energy, proposed that the radiative deexcitation of resonances near neutron binding to the various excited states could be related to the absorption of radiation by the ground state to reach an excited state. By

combining the principle of detailed balance with the idea that a "giant resonance" can be built on each excited state, it is possible to write a strength function of the form:

$$f(E_1) \equiv \frac{1}{D} \frac{\langle \Gamma_Y(E_1) \rangle_{\lambda E}}{E^3} = \frac{1}{3\pi^2 c^2 A^2} \frac{1}{E_Y} \frac{\sigma_0 \Gamma_Y^2 E_Y^2}{(E_Y^2 - E_1^2)^2 + \Gamma_Y^2 E_Y^2} \quad (3)$$

where  $f$  is in  $\text{MeV}^{-3}$ ,  $\sigma_0$  in  $\text{fm}^2$ .

It is best to quote Brink exactly on this point. He says "Now we assume that the energy dependence of the photo effect is independent of the detailed structure of the initial state so that, if it were possible to perform the photo effect on an excited state, the cross section for absorption of a photon of energy  $E$  would still have an energy dependence given by [eq. 3 above]<sup>12</sup>."

Brink proceeded to calculate the neutron resonance radiation widths with the above assumption and concluded that the model predictions were, on the average, larger than experiment by a factor of 3! I will discuss the implications of this failure in a subsequent section.

Axel<sup>13</sup> pointed out that a simple way, sufficient for some applications, to introduce the energy dependence of the photon strengths, is to use a  $\gamma$ -ray reduction factor of  $(E_Y)^5$  for E-1 radiation. For the purposes of spin-parity determinations for nuclear structure tests in heavy nuclei, this works sufficiently well to be useful over a limited excitation energy range.

#### IV. Nuclear Structure Determination

The most spectacular applications of resonance averaging have occurred in nuclear model tests. Bollinger first pointed out the unique ability of the method to ensure the determination of a complete set of states in a certain spin-parity range<sup>14</sup>. Casten and his co-workers later applied the method to establish the applicability of various symmetries in the IBA model in heavy nuclei<sup>15</sup>. The method is able, not only to establish reliable spin-parity assignments for a set of levels, but also to guarantee that all levels in a certain range have been detected.

The best example<sup>16</sup> of the method's success is  $^{168}\text{Er}$ . A plot of the 2 keV data is shown in Fig. 6 and shows a clear grouping into spin-parity bands of  $3^-, 4^-$ ;  $2^-, 5^-$ ;  $3^+, 4^+$ ; and  $2^+, 5^+$ . The probability distributions are shown in Fig. 7a-d. Excellent averaging is obtained because of the high level density of capturing states ( $\langle D \rangle \approx 4 \text{ eV}$ ). About 250 occur in the 2 keV window, while the 24 keV window contains 475 s-wave resonances and 1400 p-wave resonances. The dispersion for  $3^-, 4^-$  levels is about 14%, sufficient for accurate spin discrimination, in view of the factor of 2 intensity separation between  $(3,4)^-$  and  $(2,5)^-$ .

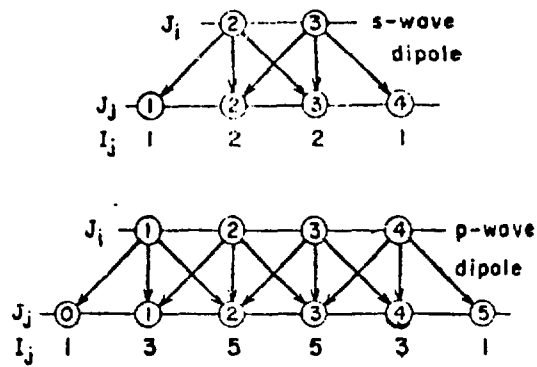


Fig. 5 Population path illustration for the intensities of final states in the  $(n,\gamma)$  reaction.

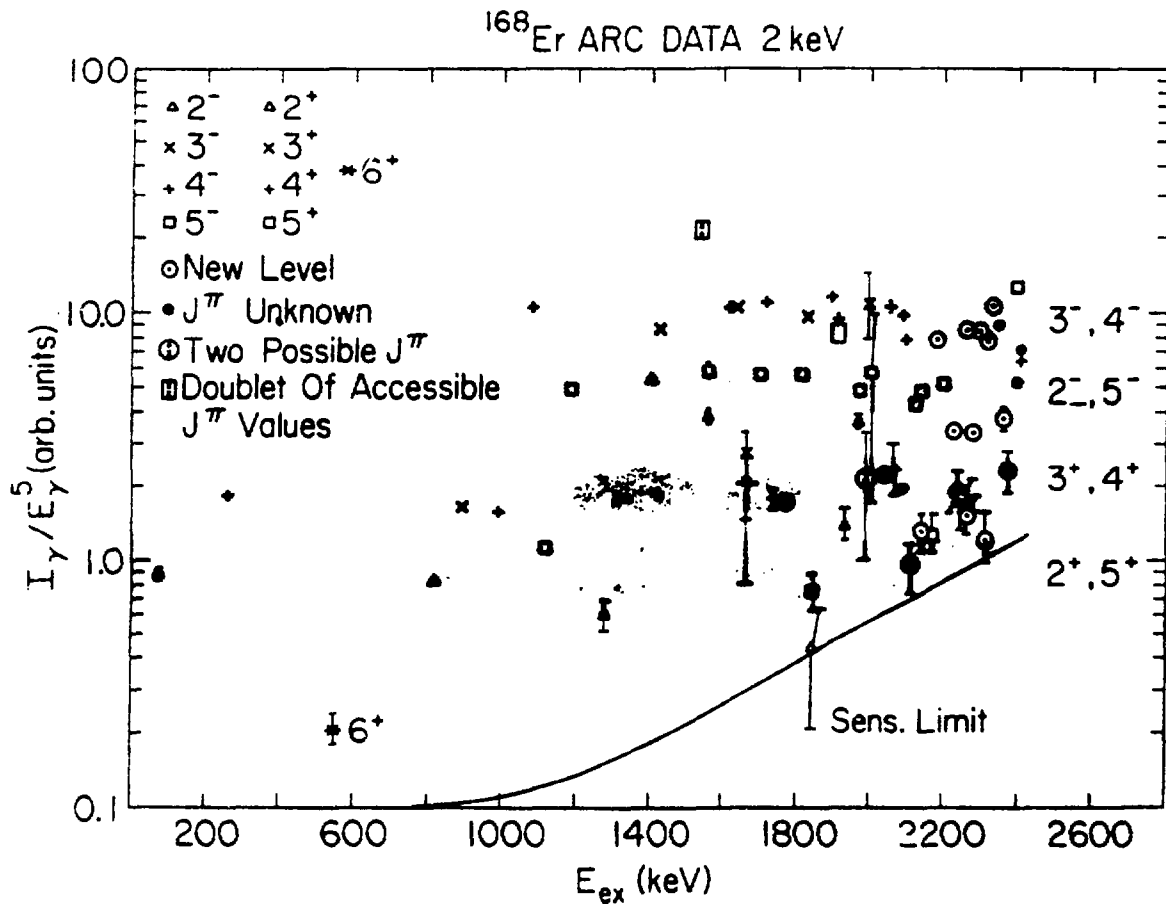


Fig. 6 Reduced 2 keV intensities for  $^{167}\text{Er}(n,\gamma)^{168}\text{Er}$  and their classification into spin-parity groupings.

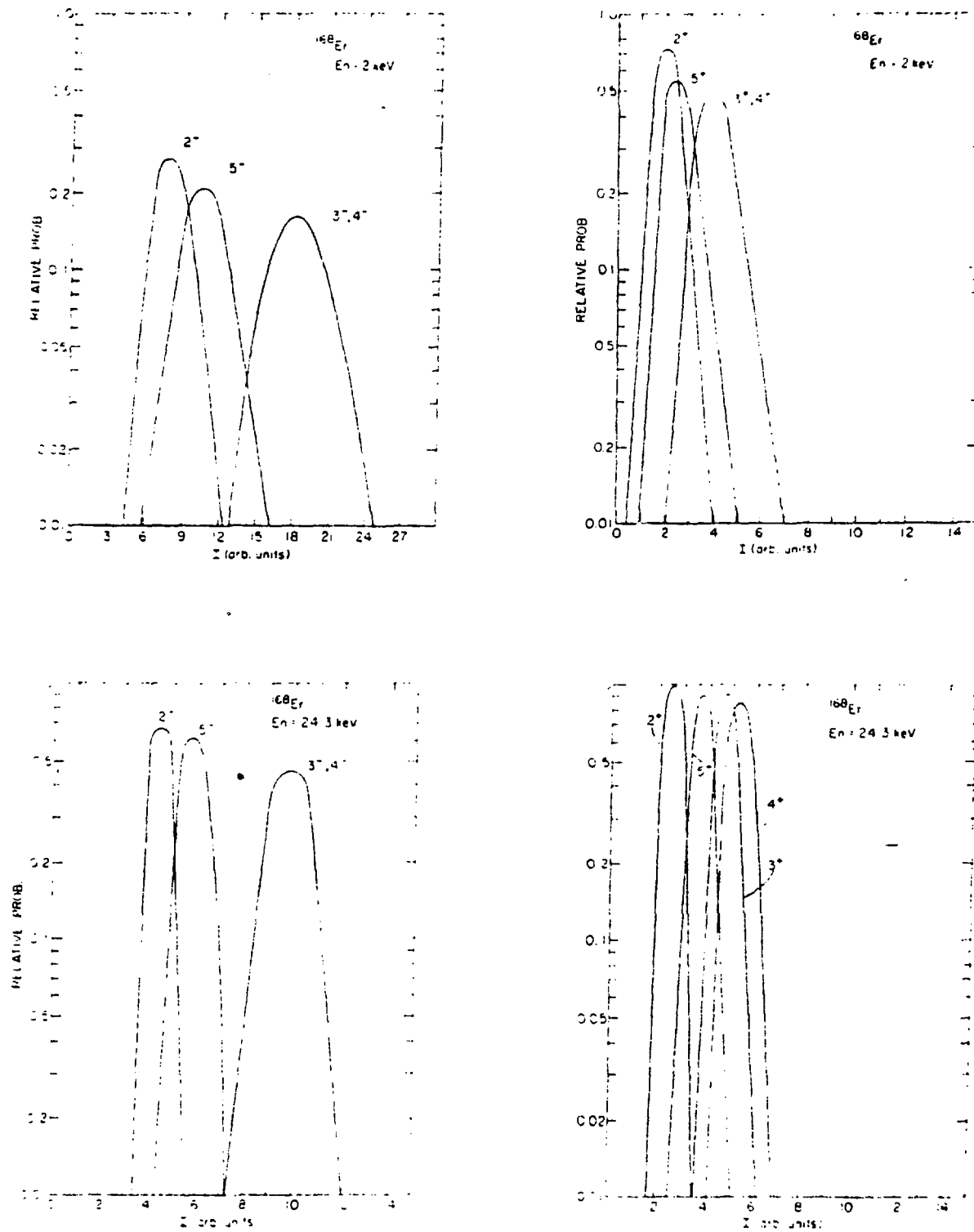


Fig. 7 Calculated distributions for the intensity distributions of the categories shown in Fig. 6.



At 24 keV, the separation ratio and the discrimination between even and odd parities is much less, as is evident from the graphs. This is due primarily to the influence of p-wave capture, which enhances the population of positive parity states. However, a useful feature of the 24 keV spectrum appears in the ratio of  $I(2)/I(24)$ , which is strongly sensitive to parity, as illustrated in Fig. 8. Thus the combination of the scandium-filtered beam, at 2 keV dominated by s-wave capture, and the iron-filtered beam, at 24.3 keV containing substantial p-wave components, results in a powerful tool for nuclear structure determinations.

#### V. An Example for Photon Strength Analysis: $^{105}\text{Pd}(n,\gamma)^{106}\text{Pd}$ Intensities

The distribution of radiative strength and the question of collective nuclear motions has been a topic of abiding interest throughout the history of nuclear physics. Resonance averaging adds an important experimental dimension to this question and provides important information at, and below, neutron binding. Resonance averaging allows 1) a clear separation of radiation according to multipolarity.  $E1$ ,  $M1$ , and to a small extent  $E2$  components are present in neutron capture. Resonance averaging allows the energy variation of the radiative strength functions to be observed over a significant energy range. With present detectors, averaged intensities can be measured over a range of about 3 MeV in typical heavy nuclides.

In this section the status of strength function measurements is described with the aid of a specific nucleus,  $^{106}\text{Pd}$ , where a wide body of  $(n,\gamma)$  and  $(\gamma,n)$  measurements are available.  $^{106}\text{Pt}$  has been the focus of recent measurements at the HFBR<sup>17</sup>.

The reduced  $\gamma$ -ray intensities observed in this 2 keV run are plotted in Fig. 9. Three groups of points are noticeable. Transitions to states of known spins and parities determine the multiplicities as indicated.

The analysis code RACA was used with the  $E1/M1$  ratio as a free parameter to predict the ratio of the population of states of known parity at 2 and 24 keV, and a best fit ratio of  $E1/M1 = 3.85 \pm 0.20$  was determined. This value was then applied to classify states of unknown parity and to assign multiplicities for all transitions.

The major part of the intensity dependence on final state spin is removed by the RACA code. Even in cases where the final state spins are not known, the differences between  $I \pm 1/2$  (where  $I$  is the target spin) and  $I \pm 3/2$  groups can be compensated by using the mean value of the correction. Finally, the code is used to correct for p-wave capture. At 2 keV the p-wave capture correction is only about 4% for  $E1$  radiation. At 24.3 keV, however, the correction for  $M1$  radiation is about 40%, because the  $M1$  population of even parity states by s-wave capture must compete against the  $E1$  population of the same states after p-wave capture. The results of RACA corrections are shown in Fig. 10, along with a sensitivity curve for the minimum observable  $\gamma$ -ray intensity.

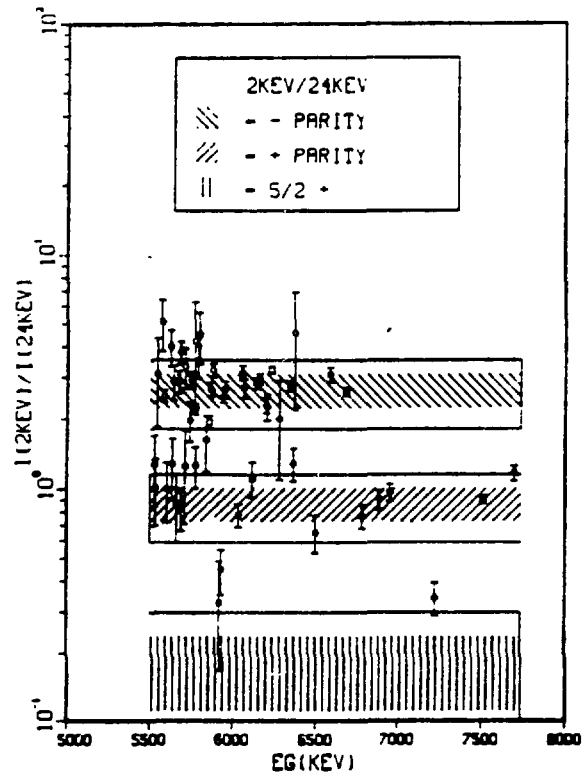


Fig. 8 The ratio of 2 keV to 24 keV intensities for  $^{168}\text{Er}$ . A marked parity dependence is evident.

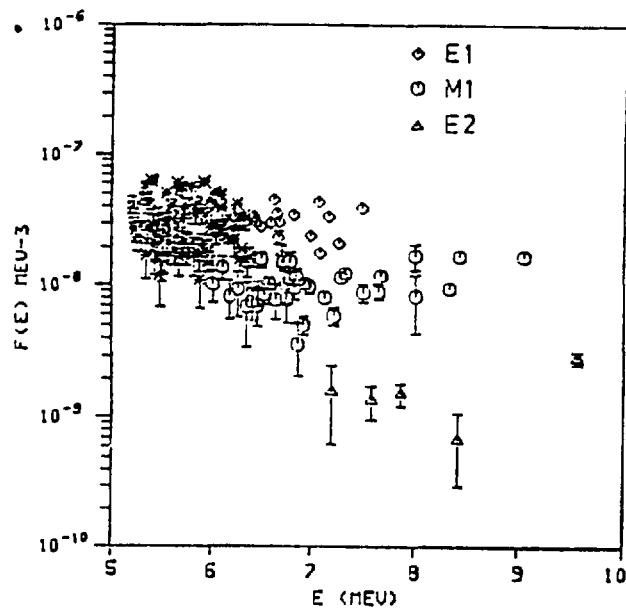


Fig. 9 Resonance-averaged intensities for  $^{105}\text{Pd}(n,\gamma)^{106}\text{Pd}$ .

The conversion of the relative intensity scale to strength function was made by referring to the absolute partial radiative widths for 10 primary transitions averaged over 9 resonances between 10 and 90 eV, as measured at the BNL fast chopper<sup>4</sup>. Values of  $\langle f(E_1) \rangle = (3.79 \pm .87) \times 10^{-8} \text{ MeV}^{-3}$  at 7.03 MeV, and  $f\langle(M1)\rangle = (1.20 \pm .26) \times 10^{-8} \text{ MeV}^{-3}$  at 7.96 MeV were obtained. The ratio  $\langle f(E_1) \rangle / f\langle(M1)\rangle$  derived from resonance data is in excellent agreement with the ratio derived from the averaged spectra.

## VI. Analysis

After decomposition of the radiative intensities into the various multipoles, one is now in a position to examine their behavior with  $\gamma$ -ray energy.

### E1 Strengths

Dover, Lemmer, and Hahne<sup>18</sup> have shown that the photoabsorption cross section can be approximated by a Lorentzian line shape, if ground state correlations are included in the shell model (the random phase approximation or RPA). It is important to stress the fact that the giant resonance damping width is energy dependent. This fact has an important effect as  $\omega (\equiv E_\gamma)$  approaches zero and it introduces a further energy dependence which is usually ignored (and is not consequential) near the resonance energy. This energy dependence was ignored by Brink in his analysis of radiation widths, and is clearly responsible for his overprediction of the widths. I do not, however, regard this as a violation of Brink's hypothesis, which as the earlier quotation shows, does not rule out such a variation.

To explicitly display this dependence, the photoabsorption cross section is written,

$$\sigma(E) = \sigma_0 \Gamma_G \frac{E^2 \Gamma(E)}{(E^2 - E_G^2)^2 + E^2 \Gamma(E)^2} \quad (4)$$

where  $\sigma_0$  is the peak cross section,  $\Gamma_G = \Gamma(E=E_G)$ , and  $E_G$  is the giant resonance energy. The dipole sum rule determines this peak cross section:

$$\sigma_0 \Gamma_G = r_0^2 (hc)^2 4\pi(NZ/A) (1+0.8x) \quad (5)$$

where  $r_0$  = classical nucleon radius ( $e^2/Mc^2$ ),  $hc = 197.3 \text{ MeV-fm}$ , and  $x$  = exchange fraction. However, it usually is preferable to use experimental values for  $\sigma_0$  and  $\Gamma_G$ , if available. The strength function is defined<sup>19</sup> as

$$f_L(E_1) = \langle \Gamma_{\nu 1f} \rangle / D_1 E^{(2L+1)} \quad (6)$$

and for E1 radiation, it can be shown that

$$f_{E1}(E_\gamma) = \frac{\sigma(E_\gamma)}{3\pi^2(\hbar c)^2 E_\gamma} \quad (7)$$

and as a result of Brink's hypothesis, one can write

$$f_{E1}(E_\gamma) = \frac{\sigma_0 \Gamma_G}{3\pi^2(\hbar c)^2} \frac{E_\gamma \Gamma(E_\gamma)}{(E_\gamma^2 - E_G^2)^2 + E_G^2 \Gamma(E_\gamma)^2} \quad (8)$$

The dependence of  $\Gamma(E_\gamma)$  can be parameterized as a power of  $E_\gamma$ . Indeed the spreading of the giant dipole particle-hole excitation into 2-particle, 2-hole states suggests that  $\Gamma(E_\gamma)$  is proportional to  $(E_\gamma)^2$ . However, a difficulty, first pointed out by Dover et al.<sup>18</sup>, is that the extrapolation of the Lorentzian function to  $E=0$  is unjustified. In a very instructive paper<sup>20</sup> Kadenskii, Markushev, and Furman examine the low energy limit and derive the correct limiting value of  $f_{E1}$  as  $E_\gamma \rightarrow 0$ . They also point out that, in addition to the  $E^2$  width dependence, one must include a contribution dependent on the temperature on which the giant resonance is built, due to quasi particle collisions. They suggest

$$\Gamma(E, T) = \frac{\Gamma_G}{E_G^2} (E^2 + 4\pi^2 T^2) \quad (9)$$

where  $T(U=B_N - E_\gamma - \Delta) = \sqrt{U/a}$ ,  $a$  = Fermi-gas level density parameter,  $\Delta$  = pairing correction,  $B_N$  = neutron binding energy. They show that for the limit  $E_\gamma \rightarrow 0$

$$f_{E1}(E_\gamma, T) = \frac{\sigma_0 \Gamma_G}{3\pi^2(\hbar c)^2} \frac{\Gamma_G}{E_G^2} \frac{(E_\gamma^2 + 4\pi^2 T^2)}{(E_\gamma^2 - E_G^2)^2} \omega_0(1 + 2/3f_1'), \quad (10)$$

here  $\omega_0$  is the shell-model energy-state difference,  $f_1'$  is a quasiparticle effective interaction strength, and the strength function  $f_{E1}$  is written  $f_{E1}(E_\gamma, T)$  to emphasize the dependence on the final state temperature  $T$ . This dependence can be viewed as a true departure from the Brink hypothesis. Kadenskii et al. assert that,

$$\frac{\omega_0(1 + 2/3f_1')}{\omega_G} \approx 0.7, \quad (11)$$

hence

$$f_{E1}(E_\gamma, T) = \frac{\sigma_0 \Gamma_G}{3\pi^2 (hc)^2} \frac{0.7 \Gamma_G}{E_G} \frac{(E_\gamma^2 + 4\pi^2 T^2)}{(E_\gamma^2 - E_G^2)^2}, \quad (12)$$

where I have rewritten the expression of Kadmenskii et al. in terms of the experimentally determined parameters  $E_G$ ,  $T_G$ . This expression, for a set of excited final states at temperature  $T$ , shows a non-zero  $f_{E1}$  at  $E \rightarrow 0$ . There is experimental evidence for this behavior from  $(n, \gamma\alpha)$  and  $(n, \gamma f)$  reactions. The references to that evidence are cited in ref. 20.

One word of caution is necessary about the  $f_{E1}(E_\gamma, T)$  above. It is valid only as  $E_\gamma \rightarrow 0$ , and fails (diverges) as  $E_\gamma \rightarrow E_G$ . Of course, neutron capture  $\gamma$  rays fall between these two limiting points and then the problem remains: what to use for  $f_{E1}$ ?

A simple alternative is simply to add  $f(0, T)$  as given by Kadmenskii et al. to the Lorentzian expression.

$$f_{E1}(E_\gamma, \Gamma) = \frac{\sigma_0 \Gamma_G}{3\pi^2 (hc)^2} \left[ \frac{E_\gamma \Gamma(E_\gamma)}{(E_\gamma^2 - E_G^2)^2 + E_\gamma^2 \Gamma(E_\gamma)^2} + \frac{0.7 \Gamma_G (4\pi^2 T^2)}{E_G^5} \right] \quad (13)$$

$$\Gamma(E_\gamma) = \Gamma_G (E_\gamma^2 + 4\pi^2 T^2) / E_G^2$$

This form is attractive because it is precisely correct in the low energy limit, and differs from the Lorentzian negligibly (1%) at the neutron binding energy. It might reasonably be expected to be valid over the whole region for neutron capture  $\gamma$  rays.

The results of various fits to the  $^{106}\text{Pd}$  E1 data are shown on Fig. 11. The four curves are 1) the Lorentzian with a fixed width,  $\Gamma_G$ ; 2) the Lorentzian with a width which varies as  $E_\gamma^{1.6}$ ; 3) the Kadmenskii et al. expression for  $U = B_n - E_\gamma$ ; and 4) the Lorentzian with the Kadmenskii width inserted. It is difficult to distinguish experimentally between 2, 3, and 4. It is interesting to note, however, the good agreement between curve 4 and the point marked "X" near 1 MeV. These points are drawn from a compilation of low energy E1  $\gamma$  rays by Endt<sup>21</sup>. They come from low lying states with an average energy of  $\approx 1$  MeV. For that case the Kadmenskii expression would be virtually identical to curve 4, and not to curve 3, which corresponds to  $U \rightarrow B_n$  as  $E_\gamma \rightarrow 0$ .

An integral condition on the various strength functions can be placed by the very accurate knowledge we have of the slow neutron radiative widths. Assuming only E1 contributions, the total radiative width,

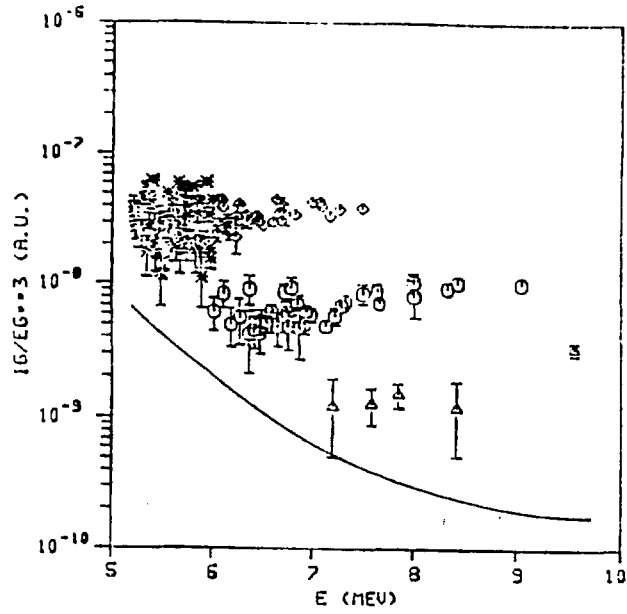


Fig. 10 The RACA-corrected (for spin-parity grouping) data of  $^{106}\text{Pd}$ .

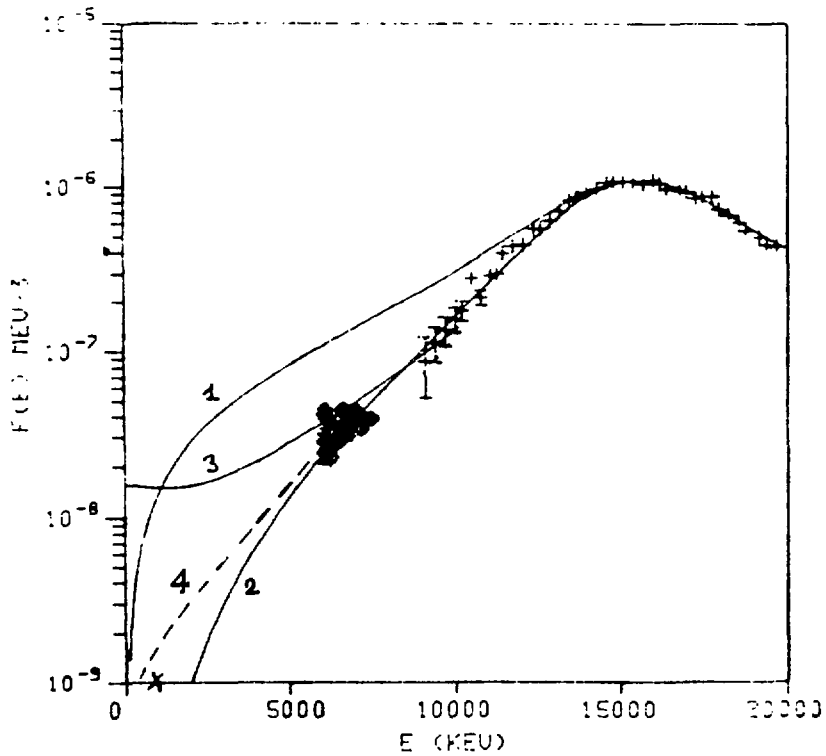


Fig. 11 The comparison of various models to the  $^{106}\text{Pd}$  E1 data: 1) Lorentzian with fixed width; 2) Lorentzian with  $\Gamma = E^{1.6}$ ; 3) Kadmenskii et al.; and 4) Lorentzian with Kadmenskii  $\Gamma$ .

$$\Gamma_Y = 3 \int_0^{B_n} f_{E1}(E_Y) \frac{\rho(B_n - E_Y - \Delta)}{\rho(B_n)} E_Y^3 dE_Y \quad (14)$$

$\Gamma_Y$  may be regarded as a weighted average of the strength function  $f_{E1}$  over the weight function  $[\rho(B_n - E_Y - \Delta)/\rho(B_n)]E_Y^3$ . The results are as follows for  $^{106}\text{Pd}$ :

1) Lorentzian, fixed width	0.431 eV
2) Lorentzian with $\Gamma = E^{1.6}$	0.046 eV
3) Kadmenskii et al.	0.170 eV
4) Lorentzian with Kadmenskii width	0.052 eV
vs	
Experiment <sup>22</sup>	0.145 ± 0.008 eV

Curve 3 gives the most acceptable value for the radiative width; the M1 contribution however has not been included.

#### M1 Strengths

The search for a collective M1 giant resonance has occupied researchers for some time<sup>23</sup>. The fragmentation of the resonance, which presumably has its origin in the shell model spin-flip transitions between  $\ell \pm 1/2$  spin-orbit partners, makes it difficult to sum the contributions of the individual fragments<sup>24</sup>.

The resonance-averaged spectral technique avoids this problem. As Fig. 10 shows, the M1 can be reasonably unambiguously separated from other multipolarities. The expectation of an M1 giant resonance is supported by (p,p') experiments on  $^{90}\text{Zr}$ ,  $^{92}\text{Zr}$ , and  $^{94}\text{Zr}$ , where a resonance energy of 8.6 to 8.8 MeV, and a resonance width of 1.5 to 1.7 MeV have been assigned<sup>25</sup>. One might expect a more severe fragmentation of the resonance in  $^{106}\text{Pd}$  from the additional nucleons added to the  $(g9/2)^{-1}, (g7/2)$  structure of Zr.<sup>26</sup>

Characteristically, M1 transitions in the mass range  $A > 90$  have been observed to vary with energy more strongly than  $E^3$ ; the only mechanism existing to support a general variation stronger than  $E^3$  is a collective resonance model.

Accordingly, the  $f_{M1}(E_Y)$  distribution has been approximated by a Lorentzian centered at 8.8 MeV, and with various values of the width  $\Gamma$ , here taken as a fixed, energy independent, parameter. The value of  $\sigma_0$ , the peak cross section, is fixed by the average of the two highest energy data points. These fits are shown in Fig. 12. A best fit is visually obtained for a width,  $\Gamma$ , of 4 MeV.

Data for M1 transitions, taken from the Endt compilation<sup>21</sup>, is also shown on the figure. This point has to be interpreted strictly in the spirit of the Brink hypothesis: the data are derived from transitions near the ground state, and not near the neutron separation energy.

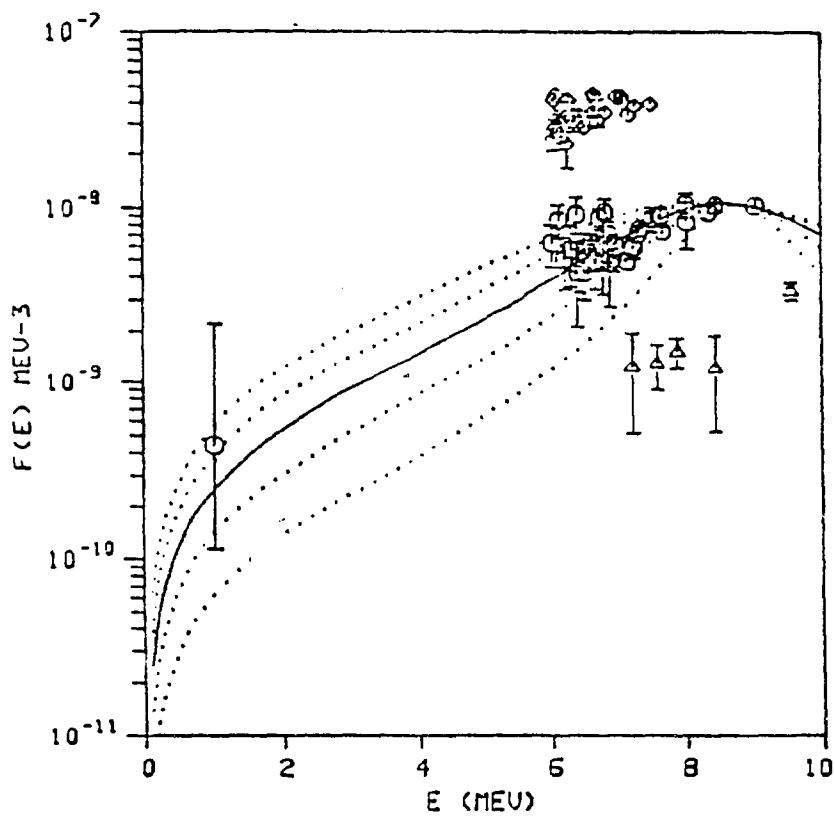


Fig. 12 The resonance averaged M1 strengths for  $^{106}\text{Pd}$  and Lorentzian curves constructed for a fixed peak cross section  $\sigma_0$ , and various widths  $\Gamma$ , from 2 to 6 MeV.



The summed strength  $\sigma_{M1}(E_R)\Gamma_R$  can be expressed<sup>27</sup> in terms of the energy weighted sum of the reduced transition probability:

$$\sigma_{M1}(E_R)\Gamma_R = 2.8 \times 10^{-3} \Sigma E B(M1) \uparrow \text{ in units of } \mu_0^2 \text{ MeV} \quad (15)$$

and related to the M1 strength function,

$$f_{M1}(E_Y) = 2.46 \times 10^{-9} \Sigma_Y B(M1) \uparrow \frac{E_Y \Gamma_R}{(E_Y^2 - E_R^2)^2 + E_Y^2 \Gamma^2} \quad (16)$$

The value obtained from the  $^{106}\text{Pd}$  data is

$$\Sigma E B(M1) \uparrow = 180 \pm 43 \mu_0^2 \text{ MeV},$$

where the error is due to averaging and the normalization against discrete resonance widths. Microscopic calculations for  $^{90}\text{Zr}$   $g_{9/2} \rightarrow g_{7/2}$  spin-flip transitions give values of 111 and 156  $\mu_0^2 \text{ MeV}$  depending on whether IPM or RPA models were used<sup>26</sup>.

### E2 Strengths

There have been few observations<sup>28</sup> of pure E2 transitions in neutron capture--too few to allow a firm basis for systematic parameterization of E2 strengths.

The present E2 data are reasonably well fit by an E2 giant resonance centered at 13.314 (taken from 63A-1/3), with a width of 4.8 MeV and a peak cross section of 2.46 mb.<sup>29-30</sup> The data are not, however, inconsistent with an energy independent single particle model.

### VII. Conclusion

The technique of resonance averaging has been shown to be a useful tool for  $(n, \gamma)$  research, particularly when care is applied in the analysis to quantify the effect of the Porter Thomas fluctuations of the contributing resonances. The method is able to locate and place a complete set of states in a certain spin-parity range. It can reliably assign average transition strengths, separated according to multipolarity, and is an excellent way to determine radiative strength functions.

### VIII. Acknowledgements

I have benefitted from useful discussions with Carl Dover, David Dowell, and, especially, with Jiri Kopecky. Research has been performed under contract DE-AC02-76CH00016 with the United States Department of Energy.

## References

1. H. A. Weidenmuller in "Neutron-Induced Reactions", Proc. of the 4th Intern. Symposium, Smolenice, D. Reidel, Dordrecht (June, 1985), p. 47.
2. L. M. Bollinger and G. E. Thomas, Phys. Rev. C2 (1970) 1951.
3. R. G. Greenwood and R. E. Chrien, Nucl. Instr. & Meth. 138 (1976) 125.
4. C. McCullagh, M. L. Stelts, and R. E. Chrien, Phys. Rev. C23 (1981) 1394.
5. M. L. Stelts and J. C. Browne, Nucl. Instr. & Meth. 133 (1976) 35.
6. A. M. Bruce, Thesis, U. of Manchester, unpublished (1986) 104.
7. L. M. Bollinger and G. E. Thomas in Proc. of the Conf. on Slow-Neutron Gamma-Ray Spectroscopy, Argonne, ANL 7282 (1966) 523.
8. J. E. Lynn, "Theory of Neutron Resonance Reactions", Clarendon Press, Oxford (1968) 227.
9. R. E. Chrien in "Neutron Capture Gamma-Ray Spectroscopy and Related Topics 1981", Conf. Ser. 62, Inst. of Phys., Bristol, London (1982) 342.
10. R. E. Chrien in ref. 1, p. 200.
11. D. M. Brink, "Some Aspects of the Interaction of Fields with Matter", Thesis, Oxford (1955).
12. Op. cit., p. 101.
13. P. Axel, Phys. Rev. 126 (1962) 671.
14. L. M. Bollinger, Phys. Rev. C3 (1971) 2071.
15. R. F. Casten, D. D. Warner, M. L. Stelts, and W. F. Davidson, Phys. Rev. Lett. 45 (1980) 1077.
16. W. F. Davidson et al., J. Phys. G7 (1981) 455.
17. J. Kopecky and R. E. Chrien, private communication, to be published.
18. C. B. Dover, R. H. Lemmer, and F.J.W. Hahne, Ann. of Phys. (NY) 70 (1972) 458.
19. G. A. Bartholomew et al., Adv. Nucl. Phys. 7 (1973) 229.
20. S. G. Kadenskii, V. P. Markushev, and V. I. Furman, Yad. Fiz. 37 (1983) 277.
21. P. M. Endt, At. Nucl. Data Tables 26 (1981) 47.
22. S. F. Mughabghab, M. Divadeenam, and N. E. Holden, "Neutron Cross Sections", Vol. 1, Academic Press, New York (1981) 46-7.
23. A. Bohr and B. Mottelson, "Nuclear Structure", Vol. II, W. A. Benjamin (1975) 636.
24. R. M. Laszewski, P. Rullhusen, S. D. Hobbit, and S. F. LeBrun, Phys. Rev. Lett. 54 (1985) 530.
25. N. Anataraman et al., Phys. Rev. Lett. 46 (1981) 1318.
26. D. Cha, B. Schweisinger, J. Wankel, and J. Speth, Nucl. Phys. A430 (1986) 321.
27. M. A. Lone in "Neutron Capture Gamma-Ray Spectroscopy", Plenum Press, New York and London (1979) 166.
28. J. Kopecky in "Capture Gamma-Ray Spectroscopy and Related Topics", AIP Conf. Proc. 125 (1985) 318.
29. F. E. Bertrand, Ann. Rev. Nucl. Sci. 26 (1976) 452.
30. W. V. Prestwich, M. A. Islam, and T. J. Kopecky, Z. Phys. A317 (1984) 210.

## **DISCLAIMER**

This report was prepared as an account of work sponsored by an agency of the United States Government. Neither the United States Government nor any agency thereof, nor any of their employees, makes any warranty, express or implied, or assumes any legal liability or responsibility for the accuracy, completeness, or usefulness of any information, apparatus, product, or process disclosed, or represents that its use would not infringe privately owned rights. Reference herein to any specific commercial product, process, or service by trade name, trademark, manufacturer, or otherwise does not necessarily constitute or imply its endorsement, recommendation, or favoring by the United States Government or any agency thereof. The views and opinions of authors expressed herein do not necessarily state or reflect those of the United States Government or any agency thereof.